Ultrafast Carrier Dynamics, Optical Amplification, and Lasing in Nanocrystal Quantum Dots

Victor I. Klimov and Moungi G. Bawendi

MRS BULLETIN REPRINT

Reprinted from Materials Research Society
MRS Bulletin, Volume 26, No. 12
December 2001

Ultrafast Carrier Dynamics, Optical Amplification, and Lasing in Nanocrystal Quantum Dots

Victor I. Klimov and Moungi G. Bawendi

Introduction

Semiconductor materials are widely used in both optically and electrically pumped lasers. The use of semiconductor quantum wells (QWs) as optical-gain media has resulted in important advances in laser technology. QWs have a two-dimensional, step-like density of electronic states that is *nonzero* at the band edge, enabling a higher concentration of carriers to contribute to the band-edge emission and leading to a reduced lasing threshold, improved temperature stability, and a narrower emission line. A further enhancement in the density of the band-edge states and an associated reduction in the lasing threshold are in principle possible using quantum wires and quantum dots (QDs), in which the confinement is in two and three dimensions, respectively. In very small dots, the spacing of the electronic states is much greater than the available thermal energy (strong confinement), inhibiting thermal depopulation of the lowest electronic states. This effect should result in a lasing threshold that is temperature-insensitive at an excitation level of only 1 electron-hole (e-h) pair per dot on average.[1] Additionally, QDs in the strong-confinement regime have an emission wavelength that is a pronounced function of size, adding the advantage of continuous spectral tunability over a wide energy range simply by changing the size of the dots.

QD lasers have been demonstrated previously using epitaxially grown nanoislands.[2,3] As predicted, these lasers show an enhanced performance, in comparison with, for example, QW lasers, and feature reduced thresholds, improved temperature stability, and high differential gain (important for achieving high modulation rates). This success has been a strong motivating force for the development of lasers based on chemically synthesized nanocrystal quantum dots (NQDs).

Direct colloidal chemical synthesis provides routine preparations of freestanding semiconductor nanoparticles (i.e., NQDs) with sub-10-nm sizes that correspond to the regime of extremely strong confinement.[4] In this size range, electronic interlevel spacings can exceed hundreds of millielectronvolts, and size-controlled spectral tunability over an energy range as wide as 1 eV can be achieved. Furthermore, improved schemes for surface passivation (e.g., by overcoating with a shell of a wide-gap semiconductor),[5] particularly well developed for CdSe NQDs, allow significant suppression of surface trapping and produce room-temperature photoluminescence (PL) quantum efficiencies as high as 50%, with emission wavelengths tunable across the entire visible spectrum. Additionally, due to their chemical flexibility, NQDs can be easily prepared as close-packed films (NQD solids) or incorporated with high densities into glasses or polymers. NQDs are, therefore, compatible with existing fiber-optic technologies and are useful as building blocks for bottom-up assembly of various optical devices, including optical amplifiers and lasers.

Despite a decade of research that provided some indications of optical-gain performance,[6,7] NQDs failed to yield lasing in numerous efforts. Difficulties in achieving lasing have often been attributed to high nonradiative carrier losses due to trapping at surface defects, a direct consequence of the large surface-to-volume ratio characteristic of sub-10-nm particles. Another concern raised in several theoretical papers is the strongly reduced efficiency of electron–phonon interactions in the case of discrete, atomic-like energy structures, which are characteristic of small dots.[8,9] For discrete spectra, the availability of pairs of electronic states satisfying energy conservation in phonon-assisted processes is drastically reduced compared with the quasicontinuous spectra of bulk materials. This deficiency has been expected to significantly lower the efficiency of carrier cooling due to phonon emission (the effect known as a "phonon bottleneck"), leading to reduced carrier flows into the lowest "emitting" states and, hence, reduced PL efficiencies. However, the difficulties anticipated due to carrier surface trapping and the "phonon bottleneck" turned out to be much less important compared with such largely unforeseen problems as nonradiative multiparticle Auger recombination[10] and interference from photoinduced absorption due to carriers trapped at NQD interfaces.

In this article, we analyze the underlying physics of processes relevant to optical amplification and lasing in strongly confined CdSe NQDs generated via organometallic colloidal reactions. Specifically, we concentrate on issues relating to intraband carrier relaxation, the effect of interface states on excited-state absorption spectra, and multiparticle Auger recombination. We show that in most common NQD/solvent systems, optical gain is suppressed by photoinduced absorption associated with carriers trapped at NQD interface states. We also find that intrinsic nonradiative Auger recombination is a dominant decay channel of optical-gain-active, doubly excited NQDs. Furthermore, we demonstrate that both of these complications can be circumvented by fabricating films of close-packed NQDs (NQD solids). These films do not show photoinduced absorption at the position of the emitting transition, and they exhibit large optical gain with a magnitude that is sufficiently high to successfully compete with multiparticle Auger recombination. NQD

films show narrow-band stimulated emission at both cryogenic and room temperatures, and the emission color is tunable with dot size. Moreover, the NQD films can be incorporated into microcavities such as microspheres that produce lasing in whispering-gallery modes, which are low-loss modes that develop in the total internal reflection regime in the near-surface area of the microsphere.

Electronic Spectra and Intraband Carrier Relaxation

Sub-10-nm NQDs exhibit atomic-like electronic spectra consisting of well-separated energy states.[11,12] In the effective-mass model,[11] conduction-band states in spherical dots are characterized by two quantum numbers: l, the angular momentum of the envelope wave function, and n, the number of the state within a series of states of the same symmetry. States with $l = 0,1,2,\ldots$ are labeled as $S,P,D,\ldots$ states. In QDs, the three lowest electron states are $1S$, $1P$, and $1D$ (Figure 1a).

A description of hole states in CdSe NQDs requires taking into account an additional quantum number, F, that is the total hole angular momentum, calculated as a sum of the Bloch-function and envelope-function momenta. The Bloch function describes carrier motion in the periodic potential of the crystalline lattice, while the envelope function describes the motion in the confinement potential of the quantum dot. In the notation for hole states, the F number is usually shown as a subscript. For example, the notation for the lowest hole state is $1S_{3/2}$. The hole states are $(2F + 1)$-fold degenerate. This degeneracy is lifted if the effects of the crystal field in a hexagonal lattice, NQD nonspherical shape, and e-h exchange interactions are taken into account, leading to a fine structure of the lowest exciton state.[13] The fine structure hole states form two groups of closely spaced levels separated by a gap that can be as large as ~100 meV in small dots (Figure 1a). This gap is observed in optical spectra as a large Stokes shift between the lowest 1S absorption maximum and a band-edge PL detected under nonresonant excitation (Figure 1b). The intense 1S absorption peak is due to a strong optical transition that couples high-energy fine structure hole states to the lowest 1S electron state, whereas the band-edge PL band is due to a weaker transition involving the lower-energy manifold of hole states (Figure 1b).

As discussed in the introduction, a large level separation in NQDs has been expected to dramatically slow down energy relaxation in comparison with bulk materials

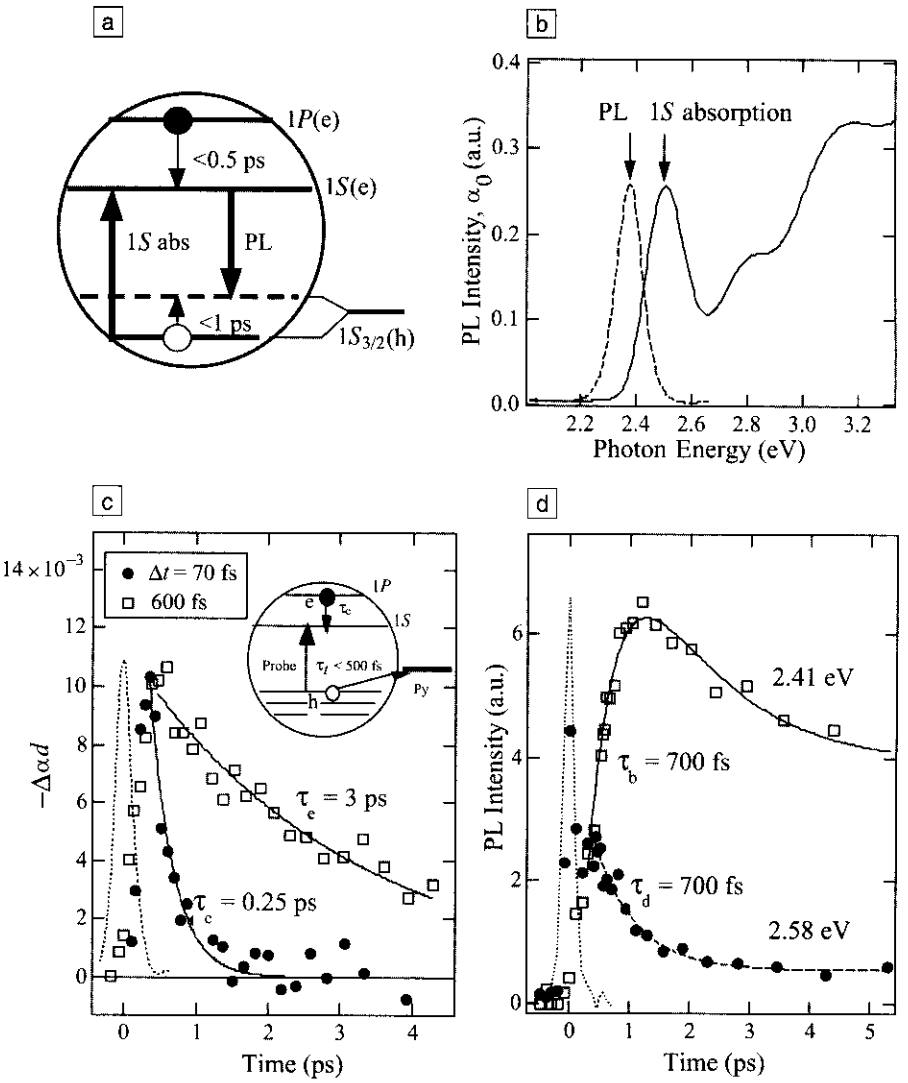

Figure 1. (a) Schematic illustration of "absorbing" (abs) and "emitting" (PL) transitions in CdSe nanocrystal quantum dots (NQDs), along with intraband relaxation processes leading to a population buildup of the "emitting" transition. (b) photoluminescence (PL) and absorption spectra of CdSe NQDs with a mean radius R = 1.2 nm (T = 300 K), illustrating a large Stokes shift between the 1S absorption peak and the PL maximum. (c) 1P-to-1S electron-relaxation dynamics detected before (solid circles) and after (open squares) hole transfer to a capping molecule; dotted line is a pump pulse tuned in resonance with the 1S–1P electron transition (Δt is the electron re-excitation time). The y-axis label, −Δαd, is the change in the absorption coefficient multiplied by the sample thickness. The inset in (c) is a schematic diagram of electron (e) and hole (h) relaxation/transfer processes. (Py is pyridine.) (d) Complementary PL dynamics detected at the positions of the "absorbing" (solid circles) and the "emitting" (open squares) transitions. Dotted line is a pump pulse used to excite PL; τ_d and τ_b are the PL decay and buildup time constants at the positions of the "absorbing" and "emitting" transitions, respectively.

due to a "phonon bottleneck." However, recent femtosecond studies of transient absorption (absorption changes induced by photogenerated carriers) demonstrate that in both chemically synthesized[14] and epitaxial[15] dots, electron relaxation is extremely fast and occurs on picosecond to subpicosecond time scales. This rapid relaxation has been attributed to an Auger-type mechanism involving intrinsic e-h interactions.[16] In this process, electron excess energy is transferred to a hole, with fast hole relaxation through the dense spectrum of valence-band states following this transfer.

Most direct studies of the role of e-h interactions on intraband relaxation have used CdSe NQDs in which e-h coupling

(separation) was controlled by varying the surface ligands.[17,18] In the presence of hole-accepting capping groups (e.g., pyridine[17,18]), the e-h coupling is strong immediately after photoexcitation (holes are inside the dot), but is reduced dramatically after hole transfer to pyridine (hole transfer time $\tau_t \approx 450$ fs; see inset in Figure 1c).[18] By re-exciting an electron between the ground (1*S*) and the first excited (1*P*) states at different stages of hole transfer and monitoring its relaxation back to the ground state, it is possible to directly evaluate the role of e-h coupling on electron-relaxation rates.[18] A more than tenfold increase (from 250 fs to 3 ps) in the electron-relaxation time, τ_e, observed after the completion of the hole transfer to the capping molecule (Figure 1c) strongly supports an electron-relaxation mechanism involving e-h interactions. Detailed studies of NQD size effects on intraband relaxation rates indicate that subpicosecond electron relaxation is observed for all dot radii between 1 nm and 4 nm.[14] Moreover, relaxation rates are enhanced in NQDs of smaller sizes, which is consistent with an Auger-type mechanism for the e-h energy transfer.

Population dynamics of hole states are more pronounced in time-resolved PL than in transient absorption.[19] The PL traces recorded at the positions of the 1*S* absorption ("absorbing" transition) and the PL maximum ("emitting" transition) show a rapid (700 fs) decay of the 1*S* emission that is complementary to the growth of the emission at the center of the PL band (Figure 1d), indicating a fast subpicosecond population buildup of the lowest "emitting" hole state. Thus, ultrafast population dynamics observed experimentally for both the lowest electron and hole quantized states suggest that optical-gain buildup should not be inhibited by the efficiency of carrier intraband relaxation.

Effect of Interface States on Excited-State Absorption Spectra

In our initial attempts to observe optical gain (optical amplification), we used CdSe NQDs in hexane solutions. To detect light amplification/attenuation, we monitored the absorption of the sample with (α) and without (α_0) pump. In absorption spectra, optical gain corresponds to $\alpha < 0$, that is, to pump-induced absorption bleaching ($\Delta\alpha = \alpha - \alpha_0 < 0$) that is greater than α_0 ($-\Delta\alpha/\alpha_0 > 1$).

In Figure 2a, we show absorption spectra of CdSe NQDs with a mean radius $R = 1.2$ nm recorded at 2 ps after excitation for progressively higher pump intensities corresponding to an increasing number of e-h pairs (N_{eh}) excited per dot (a pump photon energy is 3 eV). These spectra do not show any evidence for gain ($\alpha < 0$), even at the highest pump density of $N_{eh} = 6$. The 1*S* absorption bleaching saturates slightly below a level $|\Delta\alpha|/\alpha_0 \approx 1$, that is, right before a crossover to optical gain (Figure 2b, squares).[10,20] Such behavior indicates that the 1*S* transition is bleached by only one type of carrier (electrons), consistent with femtosecond PL data, indicating very fast hole relaxation from the "absorbing" (responsible for the 1*S* absorption) to the lower-energy "emitting" (involved in the PL transition) fine structure state (Figure 1a).

However, we do not detect gain at the position of the "emitting" transition, either. In the region of this transition, CdSe NQD/hexane samples show *increased* absorption (that is, photoinduced absorption). In contrast to 1*S* bleaching, which saturates at high pump intensities, photoinduced absorption does not show saturation (circles in Figure 2b) and, therefore, cannot be circumvented by simply increasing the excitation density.

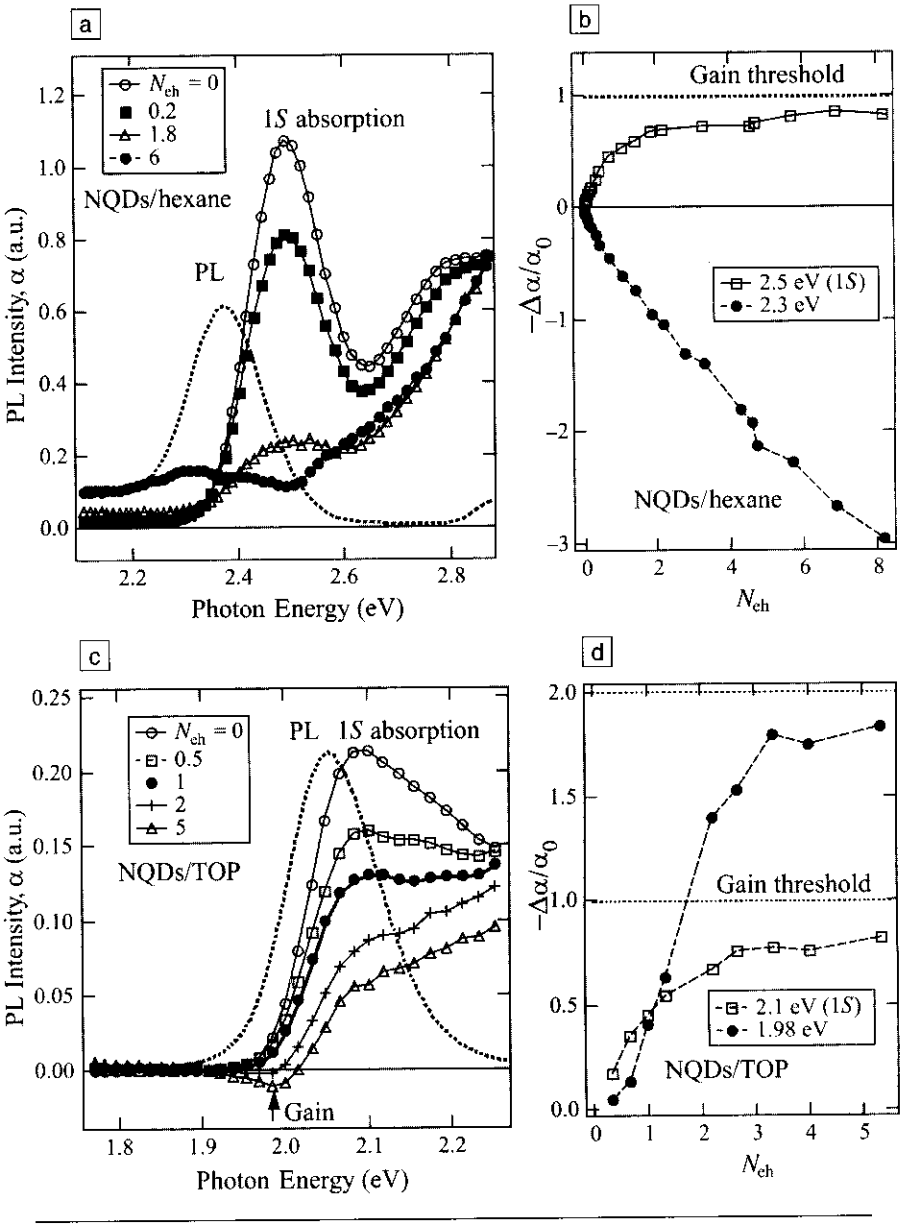

Figure 2. Pump-intensity-dependent absorption spectra of CdSe NQDs in (a) hexane and (c) trioctylphosphine (TOP) solutions, in comparison with the emission spectrum (dotted curves). Pump-intensity-dependence of normalized absorption changes at the positions of the 1S bleaching (open squares) and PL (solid circles) for (b) hexane and (d) TOP solutions. NQD mean radii are R = 1.2 nm in (a) and (b) and R = 2.3 nm in (c) and (d).

Analysis of data for NQDs in different liquid- and solid-state matrices indicates that the photoinduced absorption is dependent on the matrix material, suggesting that it is due to excited-state absorption involving carriers trapped at matrix/solvent-related interface states. Such commonly used solvents as toluene, chloroform, and heptamethylnonane (HMN) show a photoinduced-absorption band comparable in intensity to that of hexane. However, in the case of NQDs dispersed in poly(vinyl butyral), the photoinduced absorption is reduced in magnitude and is red-shifted with respect to the PL band. The strongest photoinduced-absorption suppression was observed for trioctylphosphine (TOP), one of the NQD growth solvents. A CdSe NQD/TOP sample in Figure 2c shows gain at the position of the PL band. The transition from absorption to gain occurs at carrier densities between 1 and 2 e-h pairs per dot on average (circles in Figure 2d), consistent with the 1 e-h pair theoretical threshold expected for three-dimensional, strongly confined systems.[1]

Our recent studies indicate that optical-gain performance is also sensitive to the excitation wavelength. For example, for CdSe NQD/hexane solutions, photoinduced absorption observed with a 3-eV pump can be suppressed by shifting the excitation energy toward the 1*S* absorption resonance. This suggests that excited-state absorption is generated primarily by means of ultrafast trapping from high-energy (excited) NQD states.

Despite the fact that under certain conditions, CdSe NQD solution samples show optical gain, these samples do not exhibit stimulated emission. In this case, as well as in other cases of relatively dilute NQD systems (e.g., NQD-doped glasses fabricated by high-temperature precipitation), the development of stimulated emission is inhibited by ultrafast decay of the optical gain, as described in the next section.

Multiparticle Auger Recombination and Optical-Gain Dynamics

If we model the band-edge emission in QDs using a two-level system with twofold spin-degenerate states, we find that optical gain (i.e., population inversion) begins at a carrier density of $N_{eh} = 1$, with gain saturation (i.e., complete population inversion) at $N_{eh} = 2$. These values imply that the NQD band-edge gain should be primarily due to 2 e-h pair states (i.e., due to quantum-confined biexcitons).

As our studies of multiparticle dynamics show,[10] the intrinsic decay of multiple e-h pair states in CdSe NQDs is dominated by Auger recombination. Auger recombination is a nonradiative process that leads to the recombination of e-h pairs via energy transfer to a third particle (an electron or a hole) that is re-excited to a higher energy state within the dot or outside it (Auger ionization). Auger recombination has a relatively low efficiency in bulk semiconductors, for which significant thermal energies are required to activate the effect. However, Auger decay is greatly enhanced in quantum-confined systems, in which the relaxation in momentum conservation removes an activation barrier.[21]

In QDs, Auger recombination occurs via a sequence of "quantized" steps from N, to $N - 1$, $N - 2$, ... and finally to the 1 e-h pair state, with each step characterized by a discrete exponential time constant (see Figure 3a). These quantized steps can be resolved in femtosecond transient-absorption data (Figure 3b), indicating extremely short Auger recombination times in NQDs on time scales of picoseconds to hundreds of picoseconds.[10]

For moderately well-passivated dots, nonradiative Auger relaxation of doubly excited nanoparticles (τ_2) is more efficient than the surface trapping and, therefore, imposes an *intrinsic* limit on the lifetime of

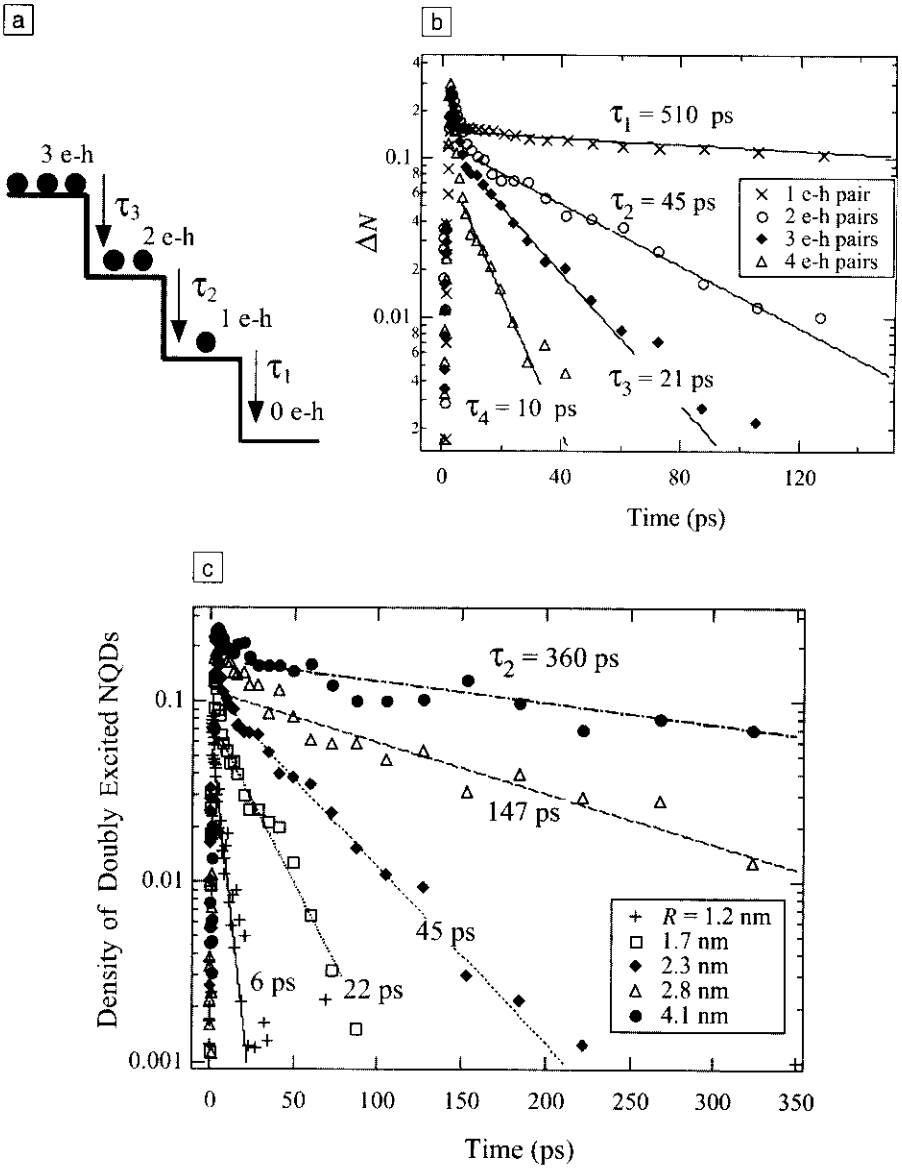

Figure 3. (a) Quantized steps in quantum-confined Auger recombination. (b) Dynamics of 1-, 2-, 3-, and 4-electron-hole (e-h) pair states extracted from transient-absorption data for CdSe NQDs with R = 2.3 nm, fit to a single exponential decay (lines); ΔN (y axis) is a density of dots in a particular multiparticle state. (c) 2 e-h pair dynamics for CdSe NQD samples with R = 1.2, 1.7, 2.3, 2.8, and 4.1 nm, fit to a single exponential decay (lines).[10]

the optical gain in strongly confined NQDs. In CdSe nanoparticles, τ_2 is strongly size-dependent ($\sim R^3$),[10] shortening from 360 ps to 6 ps as the radius decreases from 4.1 nm to 1.2 nm (Figure 3c). Because of this strong size-dependence, Auger effects, which play a minor role in large epitaxial dots, become significant in strongly confined NQDs. The dominance of the Auger effect in NQDs also implies that even poorly passivated samples could behave as well as the best samples with respect to gain and stimulated emission because, as long as trapping rates are lower than Auger rates, the 2 e-h pair lifetime is determined by the intrinsic Auger decay.

Stimulated Emission in NQDs

To overcome the problem of ultrafast gain decay, development of stimulated emission must occur on time scales that are shorter than those for Auger decay. One approach to enhancing the rate of stimulated emission is to increase the gain magnitude by increasing the dot density in the sample. Our estimations show that the stimulated emission rate exceeds that for the Auger recombination at NQD filling factors of 0.2–1%.[19] Such densities are readily achieved in close-packed NQD films (NQD solids). For example, films made of 1.3-nm NQDs capped with trioctylphosphine oxide (TOPO) have filling factors as high as 20% (a capping molecule length of 1.1 nm is assumed).

Solid-state films with thicknesses from 0.2 μm to 2 μm were fabricated on glass slides by drop-casting from hexane/octane solutions of CdSe NQDs either directly passivated with TOPO or overcoated with a shell of ZnS terminated with a TOPO layer (core-shell structures). The films exhibit random close-packing. They show optical gain at both liquid-nitrogen temperature and room temperature (Figure 4a). The gain develops at the position of the emitting transition, with a threshold that is close to the theoretical limit of 1 e-h pair per dot on average, independent of dot size. The gain threshold in terms of the pump fluence (total number of photons per pulse divided by the pump-beam cross-sectional area) scales roughly as R^{-3}, as expected from the R^3 scaling of NQD absorption cross sections at energies well above the energy gap.[22]

The NQD films also show stimulated emission as illustrated by pump-intensity-dependent emission spectra in Figure 4b (TOPO-capped CdSe NQDs with R = 2.1 nm; sample temperature 80 K). The film is optically pumped at 3 eV with 100-fs pulses; the stimulated emission is detected at the edge of the film, which acts as an optical waveguide. At pump levels of approximately 1.5 e-h pairs per dot, a sharp stimulated-emission peak develops on the low-energy side of the spontaneous-emission band. The pump-intensity-dependence of this peak (Figure 4b, inset) shows a threshold behavior that is a clear signature of optical amplification. The stimulated-emission band is spectrally tunable by changing the dot size, as expected from quantum-confinement effects (Figure 4c). For relatively large dots (R > 2 nm), observation of stimulated emission did not require the use of ZnS-overcoated dots. TOPO-capped NQDs have poorer surface passivation than core-shell structures and, hence, substantially smaller PL quantum yields. However, because in relatively large dots the Auger

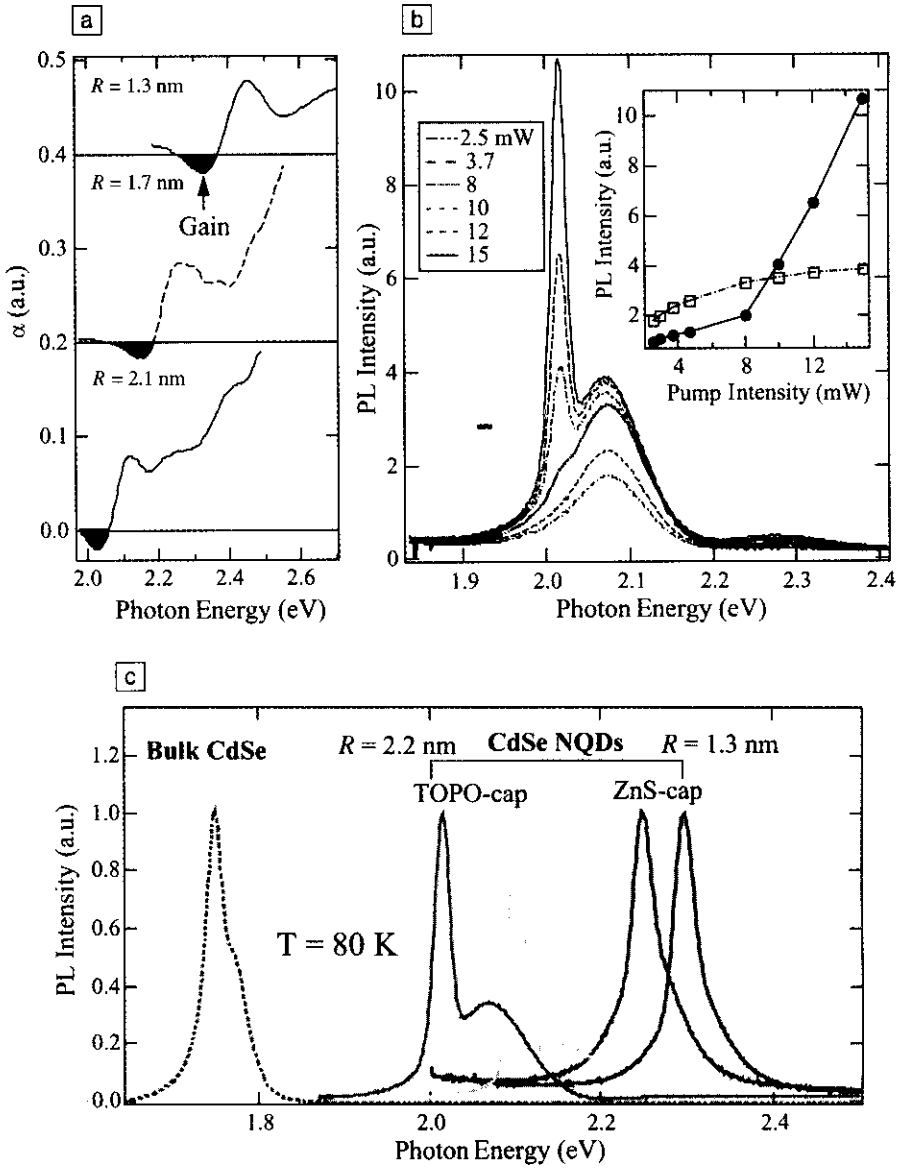

Figure 4. (a) Absorption/gain spectra of NQD films fabricated from dots with R = 1.3, 1.7, and 2.1 nm (T = 300 K); for clarity, the spectra are arbitrarily shifted along the vertical axis. The solid black areas show the region of optical gain. (b) Development of a sharp stimulated-emission band as a function of pump intensity in PL spectra of a film fabricated from trioctylphosphine oxide (TOPO)-capped CdSe NQDs with R = 2.1 nm (T = 80 K). The inset in (b) shows the superlinear intensity-dependence of the stimulated-emission peak (solid circles) compared with the sublinear dependence of the PL intensity outside this peak (open squares). (c) Size-controlled stimulated-emission spectra of films fabricated from both TOPO- and ZnS-capped CdSe NQDs compared with stimulated emission in bulk CdSe (T = 80 K). All data shown in the figure were collected using 100-fs pump pulses at 3 eV.

time scale is faster than surface trapping, both types of samples (TOPO- and ZnS-capped) showed similar properties in stimulated emission. Femtosecond PL data indicate that in TOPO-capped dots with $R < 2$ nm, hole surface trapping becomes extremely fast (time scales of <5 ps). Therefore, for these "ultrasmall" sizes, overcoating with ZnS was essential for achieving stimulated emission.

NQD samples also showed stimulated emission at room temperature. Interestingly, the same pump fluences that are used to excite room-temperature stimulated emission in CdSe NQDs are not sufficient to produce stimulated emission in bulk CdSe samples. Stimulated emission in bulk CdSe can be due to both low-threshold excitonic and high-threshold e-h plasma mechanisms. Thermal dissociation of excitons at room temperature (the exciton binding energy in CdSe is 16 meV) results in a significantly increased threshold for stimulated emission. Because of a large interlevel spacing, "quantum-confined" excitons in NQDs are more robust than bulk excitons, allowing one to excite room-temperature stimulated emission at pump levels comparable to those at cryogenic temperatures. This is an illustrative example of enhanced temperature stability in lasing applications expected for strongly confined NQDs.

NQD Microcavity Lasing

We have also demonstrated lasing from NQDs coupled to microcavities at room temperature. These results represent the first unambiguous report of lasing from highly confined colloidal nanoparticles. NQDs were assembled in a thin (<100 nm) film on the outer surface of polystyrene spheres ~10 μm in diameter. The fluorescence from the dots couples to the whispering-gallery modes of the sphere, which then acts as a microcavity for the dots. The lasing results in Figure 5 were obtained using excitation at 450 nm from a pulsed (100 fs) Ti:sapphire laser system coupled to a regenerative amplifier operating at 100 kHz. The emission from individual spheres, deposited on a cover glass, was collected using a microscope objective. The low-power spectrum in Figure 5 (lower graph) shows the broad luminescence of NQDs below lasing threshold. As the power is increased slightly above threshold, lasing into a single whispering-gallery mode is observed. As the excitation power is further increased, the number of modes that show effective feedback and lasing also increased. The inset in Figure 5 is an example of emission from another microsphere that shows both relatively broad whispering-gallery modes that are below lasing threshold and one very sharp, lone mode that emits in the lasing regime.

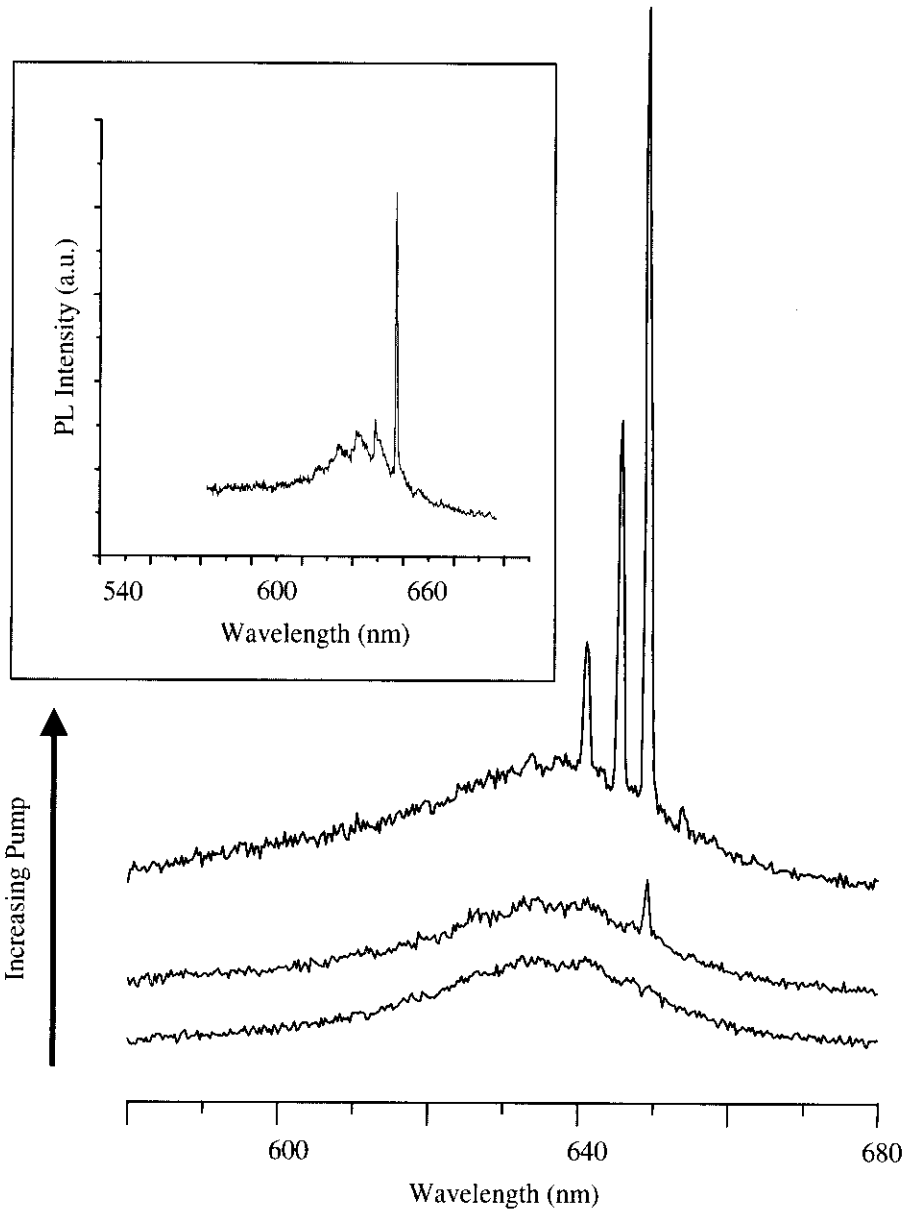

Figure 5. Spontaneous emission and whispering-gallery-mode lasing in CdSe NQDs (T = 300 K) assembled on the outer surface of ~10-μm polystyrene spheres (see text for details).

Conclusions

In this article, we analyzed optical processes relevant to optical amplification and lasing in strongly confined, sub-10-nm CdSe nanocrystal quantum dots. We observed a strong effect of surface/interface properties on optical-gain properties of NQDs. In most of the commonly used solvents (such as hexane and toluene), gain is suppressed by a strong photoinduced absorption associated with carriers trapped at solvent-related interface states. In contrast, close-packed NQD films (NQD solids) exhibit large optical gain at the position of the lowest "emitting" transition. We observed that for moderately well-passivated dots, nonradiative Auger relaxation of gain-active, doubly excited nanoparticles dominates over surface trapping and imposes an intrinsic limit on the lifetime of the optical gain. Although making it more difficult to achieve the regime of stimu-

lated emission, Auger recombination does not inherently prevent it. In particular, NQD solid-state films show optical gain of sufficient magnitude to successfully compete with multiparticle Auger recombination. These films exhibit narrow-band stimulated emission at both cryogenic and room temperatures, and the emission color is tunable with dot size. Moreover, the NQD solids can be incorporated into microcavities of different geometries (e.g., microspheres and microcapillary tubes) that produce lasing into whispering-gallery modes. These results provide a proof of principle for lasing in strongly confined colloidal nanoparticles and should motivate the development of NQD-based lasers and amplifiers over a broad spectral range.

Acknowledgments

The authors gratefully acknowledge the contributions of postdoctoral fellows and students to the work reviewed here, especially from A.A. Mikhailovsky, J.A. Hollingsworth, A. Malko, C.A. Leatherdale, H.-J. Eisler, and V.C. Sundar. This work was supported by Los Alamos Directed Research and Development funds, under the auspices of the U.S. Department of Energy. M.G. Bawendi also acknowledges partial funding from the NSF-MRSEC program under grant No. DMR-98-08941.

References

1. M. Asada, Y. Miyamoto, and Y. Suematsu, *IEEE J. Quantum Electron.* **22** (1986) p. 1915.
2. N.N. Ledentsov, V.M. Ustinov, A.Y. Egorov, A.E. Zhukov, M.V. Maksimov, I.G. Tabatadze, and P.S. Kopev, *Semiconductors* **28** (1994) p. 832.
3. N. Kistaedter, N.N. Ledentsov, M. Grundmann, D. Bimberg, V.M. Ustinov, S.S. Ruvimov, M.V. Maximov, P.S. Kopev, Z.I. Alferov, and U. Richter, *Electron. Lett.* **30** (1994) p. 1416.
4. C.B. Murray, D.J. Norris, and M.G. Bawendi, *J. Am. Chem. Soc.* **115** (1993) p. 8706.
5. M. Hines and P. Guyot-Sionnest, *J. Phys. Chem.* **100** (1996) p. 468.
6. J. Butty, Y.Z. Hu, N. Peyghambarian, Y.H. Kao, and J.D. Mackenzie, *Appl. Phys. Lett.* **67** (1995) p. 2672.
7. F. Gindele, R. Westphaeling, U. Woggon, L. Spanhel, and V. Ptatschek, *Appl. Phys. Lett.* **71** (1997) p. 2181.
8. H. Benisty, C. Sotomayor-Torres, and C. Weisbuch, *Phys. Rev. B* **44** (1991) p. 10945.
9. T. Inoshita and H. Sakaki, *Phys. Rev. B* **46** (1992) p. 7260.
10. V.I. Klimov, A.A. Mikhailovsky, D.W. McBranch, C.A. Leatherdale, and M.G. Bawendi, *Science* **287** (2000) p. 1011.
11. A.I. Ekimov, F. Hache, M.C. Schanne-Klein, D. Ricard, C. Flytzanis, I.A. Kudryavtsev, T.V. Yazeva, A.V. Rodina, and A.L. Efros, *J. Opt. Soc. Am. B* **10** (1993) p. 100.
12. D. Norris and M. Bawendi, *Phys. Rev. B* **53** (1996) p. 16338.
13. M. Nirmal, D. Norris, M. Kuno, M.G. Bawendi, A.L. Efros, and M. Rosen, *Phys. Rev. Lett.* **75** (1995) p. 3728.
14. V. Klimov and D. McBranch, *Phys. Rev. Lett.* **80** (1998) p. 4028.
15. T.S. Sosnowskii, T. Norris, H. Jiang, J. Singh, K. Kamat, and P. Bhattacharya, *Phys. Rev. B* **57** (1998) p. 9423.
16. A.L. Efros, V.A. Kharchenko, and M. Rosen, *Solid State Commun.* **93** (1995) p. 281.
17. P. Guyot-Sionnest, M. Shim, C. Matranga, and M.A. Hines, *Phys. Rev. B* **60** (1999) p. R2181.
18. V.I. Klimov, A.A. Mikhailovsky, D.W. McBranch, C.A. Leatherdale, and M.G. Bawendi, *Phys. Rev. B* **61** (2000) p. R13349.
19. V.I. Klimov, A.A. Mikhailovsky, S. Xu, A. Malko, J.A. Hollingsworth, C.A. Leatherdale, H.-J. Eisler, and M.G. Bawendi, *Science* **290** (2000) p. 314.
20. V.I. Klimov, Ch. J. Schwarz, D.W. McBranch, C.A. Leatherdale, and M.G. Bawendi, *Phys. Rev. B* **60** (1999) p. R2177.
21. D. Chepic, A.L. Efros, A. Ekimov, M. Ivanov, V.A. Kharchenko, I. Kudriavtsev, and T.V. Yazeva, *J. Lumin.* **47** (1990) p. 113.
22. V.I. Klimov, *J. Phys. Cem. B* **104** (2000) p. 6112. □